

# Collective neutrino-pair emission due to Cooper pairing of protons in superconducting neutron stars

L. B. Leinson\*

*Departamento de Física Teórica, Universidad de Valencia  
46100 Burjassot (Valencia), Spain.*

## Abstract

The neutrino emission due to formation and breaking of Cooper pairs of protons in superconducting cores of neutron stars is considered with taking into account the electromagnetic coupling of protons to ambient electrons. It is shown that collective response of electrons to the proton quantum transition contributes coherently to the complete interaction with a neutrino field and enhances the neutrino-pair production. Our calculation shows that the contribution of the vector weak current to the  $\nu\bar{\nu}$  emissivity of protons is much larger than that calculated by different authors without taking into account the plasma effects. Partial contribution of the pairing protons to the total neutrino radiation from the neutron star core is very sensitive to the critical temperatures for the proton and neutron pairing. We show domains of these parameters where the neutrino radiation, caused by a singlet-state pairing of protons is dominating.

PACS number(s): 97.60.Jd, 95.30.Cq, 13.10.+q, 13.88.+e, 71.45.-d

Keywords: Neutron star, Neutrino radiation, Superconductivity, Plasma effects

Typeset using REVTeX

---

\*On leave from: Institute of Terrestrial Magnetism, Ionosphere and Radio Wave Propagation RAS, 142092 Troitsk, Moscow Region, Russia.

## I. INTRODUCTION

When the temperature inside a neutron star core is lower than the critical temperature  $T_c$  for nucleon pairing, the nucleon matter exhibits a condensate of Cooper pairs, which has thermal excitations in the form of not paired quasi-particles. Cooper-pair formation and pair-breaking coexist in statistical equilibrium and result in additional neutrino-pair emission from the neutron star. Under certain conditions, neutrino emission due to Cooper pairing of nucleons may be sufficiently high, compared with or even larger than the emissivity of Modified Urca process in non-superfluid matter. This mechanism of energy loss was proposed by Flowers et al. many years ago [1] but have been included into cooling simulations only recently [2], [3], [4]. It was shown, that neutrino emission due to formation and breaking of Cooper pairs can accelerate the neutron star cooling.

Flowers et al. [1] have studied the neutrino-pair emissivity for the case of a singlet-state pairing of neutrons. One more independent calculation of this process was suggested by Voskresensky and Senatorov [5]. They have obtained a similar equation for the neutrino-pair emissivity, but contrary to previous authors, the expression obtained by Senatorov and Voskresensky contains the axial-vector contribution. A new calculation, performed by Yakovlev et al. [6], has confirmed that the axial-vector contribution arises actually due to relativistic effects and is negligible in the case of singlet-state pairing of neutrons.

Yakovlev et al. [6] have considered also the more probable case of a triplet-state neutron pairing.

The case of proton pairing was considered in [7]. Specifics of the proton pairing, which we are going to discuss in this paper, occurs due to a smallness of the weak vector coupling of a proton. Cooper pairing of protons take place likely in  $^1S_0$ -state [8]. When protons are treated non-relativistically, the total spin of the Cooper pair in the singlet-state is zero. By this reason, the axial-vector contribution of the proton weak current to the neutrino emissivity occurs as a relativistic correction, which, however, is found to be larger than the vector contribution due to the numerical smallness of the above weak vector constant of

protons [7].

In our paper we argue that, in spite of the smallness of the proton vector weak coupling, the latter plays an important role in the neutrino-pair radiation from pairing protons. The above inference about negligible contribution of the vector weak coupling was made on the basis of calculations which ignored electromagnetic correlations among the charged particles in a QED plasma. Actually, protons in the plasma are coupled to ambient electrons via the electromagnetic field. The electron vector weak coupling with a neutrino field is much stronger than that for protons, therefore the virtual electron cloud, associated to the medium polarization, strongly modifies the effective vector weak current of protons [9]. The collective effects caused by polarization of the electron plasma manifest themselves in the Debye volume around the proton. As the wavelength of radiated neutrino and antineutrino is much larger than the electron Debye screening distance  $D_e$  (Typically, the ratio is of the order of 10 or larger.), the induced virtual electron excitations generate neutrinos coherently with the protons undergoing the quantum transition and leads to stronger neutrino emission than that due to the direct proton interaction with a neutrino field.

In the present article we suggest the calculation of  $\nu\bar{\nu}$  radiation caused by Cooper pairing of protons in the  $^1S_0$ -state, taking into account the above collective effects. We consider the medium as consisting of neutrons, protons, and electrons. Generalization including muons is also considered.

To incorporate the electromagnetic correlations, one has to take into account exchange of photons between charged particles in the medium. For this we first consider some properties of the electromagnetic field in the plasma consisting of superconducting protons and normal degenerate electrons. In Sec. II we discuss the corresponding electromagnetic field equations, polarization functions of the medium, and derive the in-medium photon propagator. Further we demonstrate the Lagrangian to be used for weak interaction of protons and electrons with a neutrino field. Here we discuss also the problem of nuclear renormalization of the weak proton vertex. In Sec. III we derive the general formula for neutrino-pair emissivity by the use of the Optical theorem. In Sec. IV we apply the closed diagrams to calculate

the emissivity of the process in the loop approximation reproducing the result obtained by different authors, without taking into account the collective effects. In Sec. V we calculate the neutrino-pair emissivity by the use of the Random phase approximation, which incorporates the electromagnetic correlations in the medium. We derive the expression for the RPA neutrino-pair emissivity. Some practical formulae and numerical estimates are given in Sec. VI. In Sec. VII we show numerical results for some typical parameters of nuclear matter, and discuss the efficiency of neutrinos due to proton pairing. Summary and conclusion are in Sec. VIII.

In what follows we use the system of units in which  $\hbar = c = 1$  and the Boltzmann constant  $k_B = 1$ .

## II. GENERAL FORMALISM

To incorporate the collective plasma effects, one should take into account exchange of photons between charged particles in the plasma. For this we consider first the electromagnetic properties of the medium consisting of superconducting protons and normal degenerate electrons.

### A. Electromagnetic field equations

The superconducting electric current of protons and the normal electric current of electrons coexist, participating in electromagnetic oscillations of the medium. At zero temperature, the total Lagrangian density of both the complex field  $\Psi$  of proton Cooper pairs and electrons interacting with the electromagnetic field, has the form

$$L = |(\partial_\mu + 2ieA_\mu)\Psi|^2 + M_{\tilde{C}p}^2 |\Psi|^2 - \kappa |\Psi|^4 - \frac{1}{16\pi} F_{\mu\nu}^2 - j_\mu^e A^\mu + L_e^0, \quad (1)$$

where  $\kappa$  is a constant for proton-proton interaction resulting in the proton pairing, and  $M_{\tilde{C}p} \simeq 2M^*$  is the mass of the Cooper pair consisting of two protons of effective mass  $M^*$ ;  $F_{\mu\nu} = \partial_\mu A_\nu - \partial_\nu A_\mu$  is the tensor of electromagnetic field;  $j_e^\mu$  is the electron current, and

$L_e^0$  is the Lagrangian density of free electrons. As a result of spontaneous breaking of the symmetry of the ground state of the system, the vacuum expectation value of the Cooper pair field is nonzero  $\langle |\Psi|^2 \rangle = \Psi_0^2$ . Since the ground state of the system corresponds to zero spin and zero total momentum of the Cooper pair the vacuum expectation value is connected with the number density of Cooper pairs  $N_s$  by the relation  $N_s = 2E\Psi_0^2$ , where  $E \approx 2M^*$  is the energy of the Cooper pair corresponding to zero total momentum, and  $N_s$  is one-half the number density of paired protons  $N_p$ . Thus,

$$\Psi_0^2 = \frac{N_p}{8M^*}. \quad (2)$$

With allowance for the interacting with the electromagnetic field  $A_\mu$ , we represent the field of the Cooper condensate in the form

$$\Psi = \Psi_0 (1 + \rho) \exp(-2ie\phi), \quad (3)$$

where  $\rho$  and  $\phi$  are arbitrary real functions of the coordinates and time, and substitute in the Lagrangian density (1) for the fields  $\rho$  and  $\phi$ . Taking into account the following identity

$$|(\partial_\mu + 2ieA_\mu) \Psi|^2 = \Psi_0^2 (\partial_\mu \rho)^2 + 4e^2 \Psi_0^2 (A_\mu - \partial_\mu \phi)^2 (1 + \rho)^2, \quad (4)$$

we can make the gauge transformation  $A'_\mu = A_\mu - \partial_\mu \phi$ . Since the quantity  $F_{\mu\nu} = F'_{\mu\nu} = \partial_\mu A'_\nu - \partial_\nu A'_\mu$  as well as the electron current  $j_\mu^e = j'^e_\mu$  are gauge-invariant we obtain

$$L = \psi_0^2 (\partial_\mu \rho)^2 + 4e^2 \Psi_0^2 A'^2_\mu (1 + \rho)^2 + M_{Cp}^2 |\psi|^2 - \lambda |\psi|^4 - \frac{1}{16\pi} F'^2_{\mu\nu} - j^e_\mu A'^\mu + L_e^0. \quad (5)$$

As a result, the Goldstone field  $\phi$  is absorbed by the gauge transformation. Considering this and taking variations of the Lagrangian with respect to the field  $A'^\mu$ , in the linear approximation we obtain the equation

$$\partial_\nu \partial^\nu A'_\mu + 32\pi e^2 \Psi_0^2 A'_\mu = 4\pi j^e_\mu, \quad \partial^\mu A'_\mu = 0. \quad (6)$$

In the absence of the electron current ( $j^e_\mu = 0$ ), this equation would describe the eigen photon modes of mass

$$m_\gamma = \sqrt{32\pi e^2 \Psi_0^2} = \sqrt{4\pi N_p e^2 / M^*}. \quad (7)$$

This is the well-known Higgs effect. The Goldstone field  $\phi$  has been absorbed by the gauge transformation. As a consequence of this, the photon has acquired a mass and an additional longitudinal polarization.

However, the polarization of the electron plasma modifies the massive photon spectrum. In fact, in the four-momentum representation, the electron current, induced by the electromagnetic field, is  $4\pi j_\mu^e = -\pi_{\mu\nu}^{(e)} A^\nu$ . Here  $\pi_{\mu\nu}^{(e)}$  is the electromagnetic polarization tensor of the electron plasma. At finite temperature, one has to take also into account the electric current of the normal proton component consisting of non-paired proton quasi-particles. This can be described by the proton electromagnetic polarization tensor  $\pi_{\mu\nu}^{(p)}$ . One has  $4\pi j_\mu^p = -\pi_{\mu\nu}^{(p)} A^\nu$ . Thus, the equation for the field (6) takes the form (In what following we omit prime in the notation of the field):

$$K^2 A_\mu - m_\gamma^2 A_\mu - \pi_{\mu\nu}(K) A^\nu = 0, \quad K^\mu A_\mu = 0, \quad (8)$$

where the electromagnetic polarization tensor is:

$$\pi_{\mu\nu} = \pi_{\mu\nu}^{(e)} + \pi_{\mu\nu}^{(p)} \quad (9)$$

## B. Orthogonal basis

To specify the components of the polarization tensors, we select a basis constructed from the following orthogonal four-vectors

$$h^\mu \equiv \frac{(\omega, \mathbf{k})}{\sqrt{K^2}}, \quad l^\mu \equiv \frac{(k, \omega \mathbf{n})}{\sqrt{K^2}}, \quad (10)$$

where the space-like unit vector  $\mathbf{n} = \mathbf{k}/k$  is directed along the electromagnetic wave-vector  $\mathbf{k}$ . Thus, the longitudinal basis tensor can be chosen as  $L^{\rho\mu} \equiv -l^\rho l^\mu$ , with normalization  $L^\rho_\rho = 1$ . The transverse (with respect to  $\mathbf{k}$ ) components of  $\Pi^{\rho\mu}$  have a tensor structure proportional to the tensor  $T^{\rho\mu} \equiv (g^{\rho\mu} - h^\rho h^\mu + l^\rho l^\mu)$ , where  $g^{\rho\mu} = \text{diag}(1, -1, -1, -1)$  is

the signature tensor. This choice of  $T^{\rho\mu}$  allows us to describe the two remaining directions orthogonal to  $h$  and  $l$ . Therefore, the transverse basis tensor has normalization  $T_\rho^\rho = 2$ . One can also check the following orthogonality relations:  $l_\rho T^{\rho\mu} = 0$ , as well as  $k_i T^{i\mu} = 0$ , and  $K_\rho L^{\rho\mu} = K_\rho T^{\rho\mu} = 0$ .

In this basis

$$\pi^{\rho\mu}(K) = \pi_l(K) L^{\rho\mu} + \pi_t(K) T^{\rho\mu}, \quad (11)$$

where the longitudinal polarization function is defined as  $\pi_l(K) = (1 - \omega^2/k^2) \pi^{00}$  and the transverse polarization function is found to be  $\pi_t(K) = (g_{\rho\mu} \pi^{\rho\mu} - \pi_l)/2$ .

### C. Real part of polarizations

To the lowest order in the fine structure constant, the polarization tensor of the electron gas is defined as follows

$$\pi^{(e)\mu\rho}(K) = 4\pi i e^2 \text{Tr} \int \frac{d^4 p}{(2\pi)^4} \gamma^\mu \hat{G}(p) \gamma^\rho \hat{G}(p+K), \quad (12)$$

Here  $\hat{G}(p)$  is the in-medium electron Green's function. This is so-called one-loop approximation corresponding to a collisionless electron plasma.

In the case of a strongly degenerate ultrarelativistic electron plasma ( $v_F \simeq 1$ ), one has [10]:

$$\pi_l^{(e)} = \frac{1}{D_e^2} \left(1 - \frac{\omega^2}{k^2}\right) \left(1 - \frac{\omega}{2k} \ln \frac{\omega+k}{\omega-k}\right), \quad (13)$$

$$\pi_t^{(e)} = \frac{3}{2} \omega_{pe}^2 \left(1 + \left(\frac{\omega^2}{k^2} - 1\right) \left(1 - \frac{\omega}{2k} \ln \frac{\omega+k}{\omega-k}\right)\right). \quad (14)$$

Here the electron plasma frequency and the Debye screening distance are defined as

$$\omega_{pe}^2 = \frac{4}{3\pi} e^2 \mu_e^2 = \frac{4\pi n_e e^2}{\mu_e}, \quad \frac{1}{D_e^2} = 3\omega_{pe}^2, \quad (15)$$

with  $\mu_e$  and  $n_e$  being, respectively, the chemical potential and the number density of electrons. Our Eq. (13) differs from Eq. (A39) of the Ref. [10] by an extra factor  $(\omega^2/k^2 - 1)$

because our basis  $l^\mu$ ,  $h^\mu$  is different from that used by Braaten and Segel by the factor  $\sqrt{K^2}/k$ . All components of the complete tensor (11) identically coincide with that obtained in [10] for the ultrarelativistic case. In the case  $\omega > k$ , interesting for us, when the Landau damping is forbidden, the one-loop electron polarization functions  $\pi_{l,t}^{(e)}$  are real-valued.

The real part of polarization functions of the normal proton component is caused by dynamics of non-paired proton quasi-particles. For  $\omega > k$  this contribution is of the order of [11]:

$$\text{Re } \pi_l^{(p)} \sim \frac{1}{6D_p^2} \left( \frac{kV_F}{\omega} \right)^2 \ll \frac{1}{D_e^2}, \quad \frac{kV_F}{\omega} \ll 1, \quad (16)$$

where  $D_p \sim D_e$  is the Debye screening distance of protons. This proton contribution is negligible compared with the contribution of ultrarelativistic electrons. Thus, we neglect the real part of proton loops and assume that the real part of the polarization is defined by the electron contribution (13), (14) only:

$$\text{Re } \pi_l = \pi_l^{(e)}, \quad \text{Re } \pi_t = \pi_t^{(e)} \quad (17)$$

#### D. Imaginary part of polarizations

The imaginary part of polarizations, responsible for the in-medium photon decay, is caused by formation and breaking of the proton Cooper pairs. The simplest way to calculate the imaginary part of the polarization tensor is an utilizing of the unitarity relation for conversion of a photon into itself through intermediate state with two quasi-particles. This corresponds to the loop approximation for the proton polarization tensor, as shown in Fig. 1. We consider the retarded polarization tensor. At finite temperature, the unitarity relation with the intermediate state with two quasi-particles has to be written as

$$\frac{2}{\exp\left(\frac{\omega}{T}\right) - 1} \text{Im } \pi^{\mu\nu} = 4\pi e^2 \sum_{i,f} \text{Tr} (\mathcal{M}_V^\mu \mathcal{M}_V^{*\nu}), \quad (18)$$

where  $\mathcal{M}_V^\mu$  is the matrix element of the vector transition current caused by formation of the Cooper pair, i. e. due to annihilation of two proton quasi-particles of momentum-spin labels

$(\mathbf{p}, s; \mathbf{p}', -s)$  and the total four-momentum  $K$ . The summation symbol includes statistical averaging and summation over initial and final states of the background, i. e. summation over all initial  $p = (E, \mathbf{p})$  and final  $p' = (E', \mathbf{p}')$  states of the proton quasi-particle has to take into account the Pauli principle via the appropriate blocking factors, with the Fermi distribution function  $f(E) = 1/[\exp(E/T) + 1]$ .

The nonrelativistic limit can be obtained by replacing  $\bar{\psi}\gamma^0\psi \rightarrow \hat{\Psi}^+\hat{\Psi}$ ,  $\bar{\psi}\gamma_i\psi \rightarrow 0$ , where  $\hat{\Psi}$  is the secondary-quantized nonrelativistic spinor wave function of quasi-protons in superconducting matter, which is determined by the Bogoliubov transformation. The transformation for singlet-state pairing is of the form (See e.g., [12]):

$$\begin{aligned} \hat{\Psi} = & \sum_{\mathbf{p}} \exp(i\mathbf{p}\mathbf{r}) u_{\mathbf{p}} (\chi_s \hat{\alpha}_{\mathbf{p},s} + \chi_{-s} \hat{\alpha}_{\mathbf{p},-s}) \\ & + \sum_{\mathbf{p}} \exp(-i\mathbf{p}\mathbf{r}) v_{\mathbf{p}} (\chi_s \hat{\alpha}_{\mathbf{p},-s}^+ + \chi_{-s} \hat{\alpha}_{\mathbf{p},s}^+), \end{aligned} \quad (19)$$

where  $\mathbf{p}$  is a quasi-particle momentum, and

$$E = \sqrt{\epsilon^2 + \Delta^2} \quad (20)$$

is its energy with respect to the Fermi level. Near the Fermi surface, at  $|p - p_F| \ll p_F$ , one has  $\epsilon = V_F(p - p_F)$ ;  $s$  enumerates spin states;  $\Delta$  is a superfluid gap at the Fermi surface ( $\Delta \ll p_F V_F$ );  $V_F = p_F/M^*$  is the proton Fermi velocity;  $\chi_s$  is a basic spinor ( $\chi_s^+ \chi_{s'} = \delta_{ss'}$ );  $\hat{\alpha}_{\mathbf{p},s}$  and  $\hat{\alpha}_{\mathbf{p},s}^+$  are the annihilation and creation operators, respectively. The coherence factors are

$$u_{\mathbf{p}} = \sqrt{\frac{1}{2} \left(1 + \frac{\epsilon}{E}\right)}, \quad v_{\mathbf{p}} = \sqrt{\frac{1}{2} \left(1 - \frac{\epsilon}{E}\right)}. \quad (21)$$

The squared matrix element for the proton-pair vector transition has been calculated by Flowers et al. [1]

$$\sum_{\sigma} \left| \langle \mathbf{p}, \sigma; \mathbf{p}', -\sigma | \hat{\Psi}^+ \hat{\Psi} | 0 \rangle \right|^2 = 2 (u_{\mathbf{p}} v_{\mathbf{p}'} + u_{\mathbf{p}'} v_{\mathbf{p}})^2. \quad (22)$$

Thus, for non-relativistic protons we have

$$\sum_{i,f} \text{Tr} (\mathcal{M}_V^\mu \mathcal{M}_V^{*\nu}) = g^{0\mu} g^{0\nu} \int \frac{d^3 p}{(2\pi)^3} \frac{d^3 p'}{(2\pi)^3} (2\pi)^4 \delta^{(4)}(p + p' - K) f(E) f(E') 2 (u_{\mathbf{p}} v_{\mathbf{p}'} + u_{\mathbf{p}'} v_{\mathbf{p}})^2. \quad (23)$$

The dominant contribution to the integrals comes from proton momenta near the Fermi surface. As the neutrino-pair momentum is  $k \sim T_c \ll P_F$ , one can neglect  $\mathbf{k}$  in the momentum conservation  $\delta$ -function, thus obtaining  $\mathbf{p}' = -\mathbf{p}$ . After this simplification, all integrations become trivial. Assuming  $\omega > 0$ , we obtain

$$\text{Im} \pi^{00} = \frac{8e^2 p_F M^* \Delta^2}{\omega \sqrt{(\omega^2 - 4\Delta^2)}} \tanh\left(\frac{\omega}{4T}\right) \theta(\omega - 2\Delta), \quad (24)$$

where  $\theta(x)$  is the Heaviside step-function,  $M^*$  is the effective proton mass, and

$$\text{Im} \pi^{i0} = \text{Im} \pi^{0j} = \text{Im} \pi^{ij} = 0 \quad (25)$$

By the use of decomposition of the polarization tensor

$$\pi^{\rho\mu}(K) = \pi_l(K) L^{\rho\mu} + \pi_t(K) T^{\rho\mu} \quad (26)$$

we obtain finally:

$$\begin{aligned} \text{Im} \pi_l(K) &= -8 \frac{k^2}{K^2} \frac{e^2 p_F M^* \Delta^2}{\omega \sqrt{(\omega^2 - 4\Delta^2)}} \tanh\left(\frac{\omega}{4T}\right) \theta(\omega - 2\Delta), \\ \text{Im} \pi_t(K) &= 0, \end{aligned} \quad (27)$$

### E. In-medium photon propagator

The in-medium photon propagator, taking into account the medium polarization due to superconducting and normal induced currents, can be found by summation of all ring polarization diagrams. This can be performed with the aid of the Dyson equation graphically depicted in Fig. 2. Here the thin dashed line means the above massive photon, which, in the wave number-frequency space has the propagator of the standard form

$$D_0^{\mu\nu}(K) = \frac{4\pi}{K^2 - m_\gamma^2} \left( g^{\mu\nu} - \frac{K^\mu K^\nu}{m_\gamma^2} \right). \quad (28)$$

An analytical form of this equation is

$$D^{\mu\nu}(K) = D_0^{\mu\nu}(K) + \frac{1}{4\pi} D_0^{\mu\lambda}(K) \pi_{\lambda\rho}(K) D^{\rho\nu}(K). \quad (29)$$

Solution is:

$$D^{\mu\nu}(K) = D_l(K) L^{\mu\nu} + D_t(K) T^{\mu\nu} - \frac{4\pi}{m_\gamma^2} \frac{K^\mu K^\nu}{K^2}, \quad (30)$$

where the longitudinal photon propagators is:

$$D_l(K) = \frac{4\pi}{K^2 - m_\gamma^2 - \text{Re } \pi_l - i \text{Im } \pi_l}. \quad (31)$$

For  $\omega > k$ , the imaginary part of the transverse polarization vanishes, therefore the retarded transverse propagator has the form:

$$D_t(K) = \frac{4\pi}{K^2 - m_\gamma^2 - \text{Re } \pi_t + i0} \quad (32)$$

Due to conservation and gauge invariance of the vector current ( $K_\lambda \pi^{\lambda\mu} = \pi^{\lambda\mu} K_\mu = 0$ ), the last term of Eq. (30) can be omitted.

According to Eqs. (31), (32), the longitudinal and transverse electromagnetic field obey the following equations.

$$\left(-\omega^2 + k^2 + \pi_l(\omega, k) + m_\gamma^2\right) \Phi(\omega, k) = 0, \quad (33)$$

$$\left(-\omega^2 + k^2 + \pi_t(\omega, k) + m_\gamma^2\right) \mathbf{A}(\omega, k) = 0. \quad (34)$$

As  $\text{Re } \pi_{l,t} \sim \omega_{pe}^2 \gg m_\gamma^2$ , the high-frequency polarization of the medium is mostly caused by the electron gas, and the superconducting condensate of protons makes only minor correction to the eigen photon modes in the medium. The longitudinal eigen mode of oscillations has, however, a damping because of absorption of the photon by proton Cooper pairs.

One can clarify the physical nature of the photon mass by considering a static limit. In this case, presence of the superconducting condensate is crucial for the vector electromagnetic field. As  $\text{Re } \pi_t(0, k) = 0$ , Eq. (34) has the following static form

$$(k^2 + m_\gamma^2) \mathbf{A}(0, k) = 0. \quad (35)$$

This equation has no non-zero solutions for real  $k$ . Thus, the static magnetic field in the medium must vanish. This is well known the Meissner effect. The field

$$\mathbf{A}(r) = \int \frac{d^3k}{(2\pi)^3} \exp(i\mathbf{k}\mathbf{r}) \frac{4\pi\mathbf{j}_{ext}(k)}{k^2 + m_\gamma^2}, \quad (36)$$

produced in the medium by any external static electric current  $\mathbf{j}_{ext}(k)$ , is screened in a distance  $r$  as  $\exp(-m_\gamma r)$ . Therefore, the photon mass  $m_\gamma$  can be identified with the inverse penetration depth of the superconductor.

## F. Weak interactions

For convenience, we write the low-energy Lagrangian of the proton and electron interaction with a neutrino field in vacuum as follows

$$\mathcal{L}_{vac} = \frac{G_F}{\sqrt{2}} j_{(p,e)}^\mu j_\mu. \quad (37)$$

Here  $G_F$  is the Fermi coupling constant, and the neutrino weak current is of the standard form

$$j_\mu = \bar{\nu}\gamma_\mu(1 - \gamma_5)\nu. \quad (38)$$

By these notations, the weak current of a bare proton

$$j_p^\mu = \bar{\psi}\gamma^\mu(\tilde{C}_V - \tilde{C}_A\gamma_5)\psi, \quad (39)$$

where  $\psi$  stands for the proton field, is constructed with reduced constants of the vector  $\tilde{C}_V = 0.5 - 2\sin^2\theta_W \simeq 0.04$  and axial-vector  $\tilde{C}_A = 0.5g_A$  coupling;  $g_A = 1.26$ , and  $\theta_W$  is the Weinberg angle. Reserving the capital letter notations  $\tilde{C}_V$  and  $\tilde{C}_A$  for proton coupling constants, we will use, at the same time, small letters,  $c_V$ , for electron coupling constants with  $c_V = 0.5 + 2\sin^2\theta_W \simeq 0.96$  for electron neutrinos, and  $c'_V = -0.5 + 2\sin^2\theta_W \simeq -0.04$  for muon and tau neutrinos. The electron weak current is then of the form

$$j_e^\mu = \bar{u}\gamma^\mu(c_V - c_A\gamma_5)u. \quad (40)$$

Strictly speaking, the proton weak coupling vertex should be renormalized due to nucleon-nucleon correlations in nuclear matter. However, in vertices with neutral currents the nucleon correlations are weakened [5], and are negligible with respect to the plasma effects under consideration (See Appendix A). Therefore we will neglect the nuclear renormalization of the weak nucleon vertex. As for the electromagnetic vertex of the proton, its renormalization is also negligible for the matter density of interest [13]

### III. NEUTRINO EMISSIVITY

We consider the total energy which is emitted into neutrino pairs per unit volume and time. By the Optical theorem, for one neutrino flavor, the emissivity is given by the following formula:

$$Q = \frac{G_F^2}{2} \int \frac{\omega}{\exp\left(\frac{\omega}{T}\right) - 1} 2 \operatorname{Im} \tilde{\Pi}^{\mu\nu}(K) \operatorname{Tr}(j_\mu j_\nu^*) \frac{d^3 k_1}{2\omega_1(2\pi)^3} \frac{d^3 k_2}{2\omega_2(2\pi)^3}, \quad (41)$$

where the integration goes over the phase volume of neutrino and antineutrino of the total energy  $\omega = \omega_1 + \omega_2$  and the total momentum  $\mathbf{k} = \mathbf{k}_1 + \mathbf{k}_2$ . In this formula  $\tilde{\Pi}^{\mu\nu}$  is the retarded polarization tensor of the medium which has ends at the weak vertex  $(\tilde{C}_V\gamma_\mu - \tilde{C}_A\gamma_\mu\gamma_5)$ . In the absence of external magnetic fields, the parity-violating mixed axial-vector polarization does not contribute to the rate of neutrino-pair production. In fact, by inserting  $\int d^4 K \delta^{(4)}(K - k_1 - k_2) = 1$  in this equation, and making use of the Lenard's integral

$$\begin{aligned} & \int \frac{d^3 k_1}{2\omega_1} \frac{d^3 k_2}{2\omega_2} \delta^{(4)}(K - k_1 - k_2) \operatorname{Tr}(j^\mu j^{\nu*}) \\ &= \frac{4\pi}{3} (K_\mu K_\nu - K^2 g_{\mu\nu}) \theta(K^2) \theta(\omega), \end{aligned} \quad (42)$$

where  $\theta(x)$  is the Heaviside step function, we can write

$$Q = \frac{G_F^2}{48\pi^5} \int \frac{\omega}{\exp\left(\frac{\omega}{T}\right) - 1} \operatorname{Im} \tilde{\Pi}^{\mu\nu}(K) (K_\mu K_\nu - K^2 g_{\mu\nu}) \theta(K^2) \theta(\omega) d\omega d^3 k. \quad (43)$$

Since the axial-vector polarization has to be an antisymmetric tensor, its contraction in (43) with the symmetric tensor  $K_\mu K_\nu - K^2 g_{\mu\nu}$  vanishes. Thus, we can take the weak polarization tensor as the sum of vector-vector and axial-axial pieces.

#### IV. LOOP APPROXIMATION

To simplest approximation one can write

$$\tilde{\Pi}_{\text{loop}}^{\mu\nu} = \tilde{C}_V^2 \Pi_V^{\mu\nu} + \tilde{C}_A^2 \Pi_A^{\mu\nu}, \quad (44)$$

where the polarization tensors  $\Pi_{V,A}^{\mu\nu}$  are given by the same diagrams of Fig. 1, but with the ends at weak vertex. Namely, the vector-vector tensor  $\Pi_V^{\mu\nu}$  has ends at the vector weak vertex, while the axial-axial tensor  $\Pi_A^{\mu\nu}$  begins and ends at axial vertex.

Obviously, the imaginary part of the weak polarization tensor can be obtained in the same way as the imaginary part of electromagnetic polarizations. The electromagnetic polarization differs from the weak vector-vector polarization only by a constant factor  $4\pi e^2$ , which is included in the definition of the electromagnetic tensor. Thus,

$$\text{Im } \Pi_V^{\mu\nu} = \frac{1}{4\pi e^2} \text{Im } \pi^{\mu\nu}. \quad (45)$$

By the use of decomposition of the vector weak polarization tensor

$$\Pi_V^{\rho\mu}(K) = \Pi_l(K) L^{\rho\mu} + \Pi_t(K) T^{\rho\mu} \quad (46)$$

we obtain

$$\begin{aligned} \text{Im } \Pi_l(K) &= -\frac{2}{\pi} \frac{k^2}{K^2} \frac{p_F M^* \Delta^2}{\omega \sqrt{(\omega^2 - 4\Delta^2)}} \tanh\left(\frac{\omega}{4T}\right) \theta(\omega - 2\Delta), \\ \text{Im } \Pi_t(K) &= 0, \end{aligned} \quad (47)$$

As mentioned above, in the case of non-relativistic protons, the total spin of the Cooper pair in the  $^1S_0$ -state is zero, therefore the axial contribution is proportional to a small parameter  $V_F^2$ . However, due to numerical smallness of the proton weak vector coupling constant

the axial contribution should be taken into account. Considering the non-relativistic axial-vector current of the proton to accuracy  $V_F$  we have to include also the relativistic correction to its temporal component by replacing  $\bar{\psi}\gamma^0\gamma^5\psi \rightarrow \hat{\Psi}^+\hat{\phi} + \hat{\phi}^+\hat{\Psi}$ ,  $\bar{\psi}\gamma_i\gamma^5\psi \rightarrow \hat{\Psi}^+\sigma_i\hat{\Psi}$ . Here the proton bispinor  $\psi$  is presented as combination of an upper spinor  $\hat{\Psi}$  and lower spinor  $\hat{\phi} = -i\sigma_i\nabla_i\hat{\Psi}/(2M)$ , where  $M$  is the bare proton mass, and  $\sigma_i$  are the Pauli matrices.

Direct calculation shows that the tensor  $I_A^{\mu\nu} \equiv \sum_{\sigma} (\mathcal{M}_A^{\mu}\mathcal{M}_A^{*\nu})$  is diagonal, with two nontrivial elements [7]:

$$\begin{aligned} I_A^{00} &= (u'v + v'u)^2 \frac{|\mathbf{p} - \mathbf{p}'|^2}{2M^2}, \\ I_A^{11} &= I_A^{22} = I_A^{33} = 2(u'v - v'u)^2. \end{aligned} \quad (48)$$

The subsequent calculations with the help of the formula

$$\frac{2}{\exp\left(\frac{\omega}{T}\right) - 1} \text{Im} \Pi_A^{\mu\nu} = \sum_{i,f} \text{Tr} (\mathcal{M}_A^{\mu}\mathcal{M}_A^{*\nu}), \quad (49)$$

yield

$$\text{Im} \Pi_A^{00} = \frac{2}{\pi} \frac{M^{*2}}{M^2} V_F^2 \frac{p_F M^* \Delta^2}{\omega \sqrt{(\omega^2 - 4\Delta^2)}} \tanh\left(\frac{\omega}{4T}\right) \theta(\omega - 2\Delta) \quad (50)$$

$$\text{Im} \Pi_A^{11} = \text{Im} \Pi_A^{22} = \text{Im} \Pi_A^{33} = \frac{1}{3\pi} k^2 V_F^2 \frac{p_F M^* \Delta^2}{\omega^3 \sqrt{\omega^2 - 4\Delta^2}} \tanh\left(\frac{\omega}{4T}\right) \theta(\omega - 2\Delta) \quad (51)$$

Once the imaginary part of the polarization is calculated, one can evaluate the  $\nu\bar{\nu}$  emissivity as indicated in Eq. (43). By the use of the Eqs. (44), (46), (47), (50), (51)) we obtain

$$Q^{\text{loop}} = Q_V^{\text{loop}} + Q_A^{\text{loop}}, \quad (52)$$

where the vector weak coupling contribution is

$$Q_V^{\text{loop}} = \frac{16}{15\pi^5} \mathcal{N}_{\nu} G_F^2 \tilde{C}_V^2 p_F M^* \Delta^7 \int_1^{\infty} \frac{z^5}{(\exp(yz) + 1)^2 \sqrt{(z^2 - 1)}} dz, \quad (53)$$

with  $y = \Delta/T$  and  $\mathcal{N}_{\nu}$  being the number of neutrino flavors. The axial-vector coupling gives:

$$Q_A^{\text{loop}} = \left( \frac{M^{*2}}{M^2} + \frac{11}{42} \right) V_F^2 \frac{\tilde{C}_A^2}{\tilde{C}_V^2} Q_V^{\text{loop}} \quad (54)$$

This result reproduces the emissivity obtained in [1] and [7]. In spite of the fact that the Fermi velocity of protons is small, the axial term (54) is typically larger, than the vector term (53) due to  $\tilde{C}_A^2/\tilde{C}_V^2 \gg 1$ .

## V. RANDOM-PHASE APPROXIMATION

### A. RPA polarizations

In the above loop approximation we ignored electromagnetic correlations among the charged particles in a QED plasma. To incorporate the collective plasma effects, one can use the Random phase approximation (RPA). In the case under consideration, the RPA means a summation of all ring diagrams connected by the line of a massive photon. One can perform the above summation with the aid of the in-medium photon propagator  $D_{\mu\nu}(K)$ , which is solution of the Dyson equation collecting all ring particle-hole diagrams, responsible for the electromagnetic polarization of the medium, as shown in Fig. 2. In this way, the graphical representation of the RPA weak polarization tensor  $\tilde{\Pi}_V^{\mu\nu}$  is of the form shown in Fig. 3. Here the first term describes the contribution, which comes directly from the pairing protons. The other terms are caused by the plasma polarization. Analytically one has:

$$\begin{aligned} \text{Im } \tilde{\Pi}_l^{\text{RPA}} = \frac{1}{4\pi e^2} \left[ \tilde{C}_V^2 \text{Im } \pi_l + \frac{1}{4\pi} \left( c_V^2 \text{Im } D_l (\text{Re } \pi_l)^2 \right. \right. \\ \left. \left. - 2\tilde{C}_V c_V \text{Im } \pi_l \text{Re } D_l \text{Re } \pi_l - \tilde{C}_V^2 (\text{Im } \pi_l)^2 \text{Im } D_l \right) \right]. \end{aligned} \quad (55)$$

Here we took into account the fact that

$$\text{Re } \pi_l^{(p)} = \text{Im } \pi_l^{(e)} = 0 \quad (56)$$

as discussed above. An extra factor  $(4\pi e^2)^{-1}$  appears in Eq. (55) because we replaced weak polarization tensors by electromagnetic tensors of the plasma. One more factor  $(4\pi)^{-1}$  appears because the factor  $4\pi$  is traditionally included into the definition of electromagnetic

polarization tensors. The minus sign, in front of terms, which are proportional to  $\tilde{C}_V c_V$ , is due to the fact that those diagrams include the proton charge  $e > 0$  at one of electromagnetic vertices of the virtual photon, and the electron charge  $-e$  at the opposite end. The corresponding factor  $e^2$  which appears accordingly to the diagrams with a photon line, is also included into the definition of polarization tensors. For the transverse weak polarization we obtain

$$\text{Im } \tilde{\Pi}_t^{\text{RPA}} = \frac{c_V^2}{8\pi^2 e^2} \text{Im } D_t (\text{Re } \pi_t)^2. \quad (57)$$

By replacing the photon propagators by their explicit expressions (31), (32) we obtain:

$$\text{Im } \tilde{\Pi}_l^{\text{RPA}} = \frac{\text{Im } \pi_l}{4\pi e^2} \left[ \frac{\tilde{C}_V^2 (K^2 - m_\gamma^2 - \text{Re } \pi_l)^2}{(K^2 - m_\gamma^2 - \text{Re } \pi_l)^2 + (\text{Im } \pi_l)^2} - \frac{2\tilde{C}_V c_V (K^2 - m_\gamma^2 - \text{Re } \pi_l) \text{Re } \pi_l}{(K^2 - m_\gamma^2 - \text{Re } \pi_l)^2 + (\text{Im } \pi_l)^2} + \frac{c_V^2 (\text{Re } \pi_l)^2}{(K^2 - m_\gamma^2 - \text{Re } \pi_l)^2 + (\text{Im } \pi_l)^2} \right]. \quad (58)$$

$$\text{Im } \tilde{\Pi}_t^{\text{RPA}} = \frac{c_V^2}{4\pi e^2} (\text{Re } \pi_t)^2 \delta (K^2 - m_\gamma^2 - \text{Re } \pi_t) \quad (59)$$

The imaginary part of the transverse polarization corresponds to the transverse eigen photon mode, which has the dispersion defined by Eq. (34). The eigen-mode frequency  $\omega_t(k)$  is larger than the plasma frequency of electrons. Thus, the term  $\text{Im } \tilde{\Pi}_t$  describes the contribution from the decay of real transverse photon of energy  $\omega_t(k) > \omega_{pe} \gg T_c$ . At temperatures  $T < T_c \ll \omega_{pe}$ , the number of such photons in the medium is exponentially suppressed, therefore this term can be neglected.

By the same reason we can neglect the RPA corrections to the axial medium polarization. Detailed consideration shows that these corrections occur due to exchange of transverse photons between charged particles in the plasma. As the imaginary part of the transverse photon is the delta-function, the RPA corrections to the axial polarization are of the form

$$\delta \text{Im } \tilde{\Pi}_t^{\text{RPA}} = \frac{c_V^2}{4\pi e^2} (\text{Re } \pi_{AV})^2 \delta (K^2 - m_\gamma^2 - \text{Re } \pi_t), \quad (60)$$

where  $\text{Re } \pi_{AV}$  is the mixed axial-vector polarization function of the electron plasma. Obviously such a correction is caused by the transverse plasmon decay. Thus, we take

$$\left(\text{Im } \tilde{\Pi}_A^{\mu\nu}\right)^{\text{RPA}} = \left(\text{Im } \tilde{\Pi}_A^{\mu\nu}\right)^{\text{loop}} \quad (61)$$

Further, as the polarization function  $\pi_l \sim \omega_{pe}^2$ , we can neglect  $K^2 \sim T_c^2 \ll \omega_{pe}^2$  in Eq. (58). By replacing also the common factor as specified by Eq. (45) we obtain:

$$\text{Im } \tilde{\Pi}_l^{\text{RPA}} = \text{Im } \Pi_l \left[ \tilde{C}_V^2 \frac{(m_\gamma^2 + \text{Re } \pi_l)^2}{(m_\gamma^2 + \text{Re } \pi_l)^2 + (\text{Im } \pi_l)^2} + 2c_V \tilde{C}_V \frac{(m_\gamma^2 + \text{Re } \pi_l) \text{Re } \pi_l}{(m_\gamma^2 + \text{Re } \pi_l)^2 + (\text{Im } \pi_l)^2} + c_V^2 \frac{(\text{Re } \pi_l)^2}{(m_\gamma^2 + \text{Re } \pi_l)^2 + (\text{Im } \pi_l)^2} \right], \quad (62)$$

where the loop polarizations are defined in Eqs. (47), (27), and (13); and  $m_\gamma$ , given by Eq.(7), is the mass acquired by a photon in the superconductor due to the Higgs effect. As noticed above, this mass can be identified with the inverse penetration depth of the superconductor. If to eliminate the plasma polarization by taking formally  $\pi_l \rightarrow 0$  then Eq. (62) reproduces the result obtained in the loop approximation. However, the plasma polarization strongly modifies that result.

The first term in the brackets of Eq. (62) is the summarized contribution of two diagrams of the Fig. 3, which are proportional to  $\tilde{C}_V^2$ . This term is always less than unity. This means, that ambient protons screen the weak vector interaction of the pairing protons with a neutrino field.

Let us estimate relative contributions of different terms in Eq. (62). According to Eqs. (7) and (15), the penetration depth of the superconductor is typically larger than the electron Debye screening distance, i.e.  $m_\gamma^2 \ll D_e^{-2}$ . Thus,  $m_\gamma^2 \lesssim |\text{Re } \pi_l|$ , and therefore  $|m_\gamma^2 + \text{Re } \pi_l| \sim |\text{Re } \pi_l|$ .

For electron neutrinos one has  $\tilde{C}_V^2/c_V^2 \simeq 1.74 \times 10^{-3}$  and  $\tilde{C}_V/c_V \simeq 4.17 \times 10^{-2}$ . Thus, for electron neutrinos, the first two terms in Eq. (62) are small compared with the term, which is proportional to  $c_V^2$ . For muon and tauon neutrinos all the terms are about  $10^{-3}$  of the leading contribution for electron neutrinos. Numerical tests have shown that, to accuracy

less than one percent, the vector contribution to the emissivity can be described by the leading term which is proportional to  $c_V^2$ . Notice that relativistic corrections, which we do not take into account, are of order  $V_F^2$  ( $V_F^2 \simeq 0.06$  for a  $\beta$ -equilibrium nuclear matter of the density  $\rho = 2\rho_0$ ). To this accuracy, the above small terms must be ignored. Thus we obtain the following analytic expression for the imaginary part of the vector-vector RPA tensor

$$\text{Im } \tilde{\Pi}_l^{\text{RPA}} \simeq c_V^2 \text{Im } \Pi_l \frac{(\text{Re } \pi_l)^2}{(m_\gamma^2 + \text{Re } \pi_l)^2 + (\text{Im } \pi_l)^2}. \quad (63)$$

This approximation corresponds to the diagram with two electron loops in Fig. 3.

### B. Including muons

When the chemical potential of electrons  $\mu_e$  is larger than the muon mass  $m_\mu$ , the  $\beta$ -equilibrium nuclear matter contains muons. Generalization of Eq. (63) to the case of p, e,  $\mu$  plasma is obvious. One has to add the corresponding diagrams with muon loops both to the Dyson's equation for the photon propagator and to the RPA polarization tensor. This yields

$$\sum_{\nu_e, \nu_\mu, \nu_\tau} \text{Im } \tilde{\Pi}_l^{\text{RPA}} \simeq c_V^2 \text{Im } \Pi_l \left[ \frac{(\text{Re } \pi_l^{(e)})^2 + 2 (\text{Re } \pi_l^{(\mu)})^2}{(m_\gamma^2 + \text{Re } \pi_l^{(e)} + \text{Re } \pi_l^{(\mu)})^2 + (\text{Im } \pi_l)^2} \right], \quad (64)$$

where the muonic polarization function is

$$\pi_l^{(\mu)} = \frac{1}{D_\mu^2} \left( 1 - \frac{\omega^2}{k^2} \right) \left( 1 - \frac{\omega}{2kv_F} \ln \frac{\omega + kv_F}{\omega - kv_F} \right). \quad (65)$$

In Eq. (64), the fact is taken into account that the weak vector coupling constant for a muon radiating muonic, and tauon neutrinos is the same as that for an electron radiating electron neutrinos. By this reason the muonic polarization function comes in the numerator of Eq. (64) with the factor of 2. The muonic Fermi velocity

$$v_F = \frac{\sqrt{\mu_\mu^2 - m_\mu^2}}{\mu_\mu}, \quad (66)$$

and the Debye screening distance

$$D_\mu^{-2} = 3 \frac{4\pi n_\mu e^2}{\mu_\mu v_{F\mu}^2} = \frac{4}{\pi} e^2 (\mu_\mu^2 - m_\mu^2)^{1/2} \mu_\mu. \quad (67)$$

depend on the muonic chemical potential  $\mu_\mu$ .

Numerical evaluation under condition of chemical equilibrium  $\mu_\mu = \mu_e$  shows (see Fig. 7) that muons introduce a minor correction to neutrino emissivity.

### C. RPA emissivity

By inserting the imaginary part of the vector-vector RPA polarization tensor

$$\text{Im} \left( \tilde{\Pi}_V^{\text{RPA}} \right)^{\mu\nu} = \text{Im} \tilde{\Pi}_l^{\text{RPA}} L^{\mu\nu} \quad (68)$$

to the emissivity equation

$$Q_V^{\text{RPA}} = \frac{G_F^2}{48\pi^5} \int \frac{\omega}{\exp\left(\frac{\omega}{T}\right) - 1} \text{Im} \left( \tilde{\Pi}_V^{\text{RPA}} \right)^{\mu\nu} (K_\mu K_\nu - K^2 g_{\mu\nu}) \theta(K^2) \theta(\omega) d\omega d^3k, \quad (69)$$

we obtain the following vector contribution to emissivity:

$$Q_V^{\text{RPA}} = -\frac{G_F^2 c_V^2}{12\pi^4} \int_{2\Delta}^{\infty} d\omega \int_0^\omega dk k^2 \frac{\omega(\omega^2 - k^2)}{\exp\left(\frac{\omega}{T}\right) - 1} \text{Im} \Pi_l \frac{(\text{Re} \pi_l)^2}{(m_\gamma^2 + \text{Re} \pi_l)^2 + (\text{Im} \pi_l)^2}. \quad (70)$$

According to above discussion  $Q_V^{\text{RPA}}$ , given by this formula, is the  $\nu\bar{\nu}$  emissivity of ambient electrons perturbed by the proton quantum transition. Therefore it is proportional to the square of the electron vector weak coupling constant, and vanishes when the proton energy gap is closed, because  $\text{Im} \Pi_l(\Delta = 0) = 0$ .

Replacing the polarization functions by their explicit expressions (47), (27), and (13) we finally obtain:

$$Q_V^{\text{RPA}} = \frac{16}{15\pi^5} G_F^2 c_V^2 p_F M^* \Delta^7 \int_1^\infty dz \frac{z^7 \sqrt{z^2 - 1}}{[\exp(zy) + 1]^2} \int_0^1 dx \frac{5x^4 (1 - x^2)^2 \varphi^2(x)}{z^2 (z^2 - 1) (1 - x^2)^2 (\varphi(x) - \lambda x^2)^2 + x^8 \tanh^2(zy/2) \eta^2} \quad (71)$$

with

$$\varphi(x) = (1 - x^2) \left( 1 - \frac{1}{2x} \ln \frac{1+x}{1-x} \right). \quad (72)$$

Additionally to the temperature and the energy gap, the emissivity caused by the vector weak coupling depends substantially on two new parameters which does not appear in the loop approximation. The parameter

$$\lambda = m_\gamma^2 D_e^2 = \frac{\mu_e n_p N_p (T/T_c)}{3M^* n_e n_p} \quad (73)$$

is the squared ratio of the electron Debye screening distance to the penetration depth of the superconductor. The latter equality follows from (15) and (7). Here  $n_e$  is the number density of electrons;  $n_p$  is the total proton number density, and  $N_p (T/T_c)$  is the number density of paired protons. In the case of p, e-plasma one has  $n_p = n_e$ . Typically  $\lambda \sim 0.05 \div 0.1$ . The second parameter is  $\eta = 2 e^2 p_F M^* D_e^2$ , which can be written in the following form

$$\eta = \frac{\pi D_e^2}{2 D_p^2}, \quad (74)$$

where

$$\frac{1}{D_p^2} = 3 \frac{4\pi e^2 n_p}{M V_F^2} \quad (75)$$

is the inverse Debye screening distance of protons. The parameter  $\eta$  is typically about one.

The temperature dependence of the emissivity enters by means of parameter

$$y = \frac{\Delta(T)}{T} = \frac{\Delta(0)}{T_c} \frac{\Delta(\tau)}{\tau \Delta(0)} \quad (76)$$

with  $\tau = T/T_c$ . For a singlet-state pairing  $\Delta(0)/T_c = 1.76$  (See e.g. [12]), therefore the function  $y$  depends on the dimensionless temperature  $\tau$  only. Thus, the emissivity (71), in  $[\text{erg s}^{-1} \text{ cm}^{-3}]$ , can be written as

$$Q_V^{\text{RPA}} = 1.17 \times 10^{21} c_V^2 \left(\frac{M^*}{M}\right)^2 V_F \left(\frac{T_c}{10^9 K}\right)^7 \tau^7 y^7 \int_1^\infty dz \frac{z^7 \sqrt{z^2 - 1}}{[\exp(zy) + 1]^2} \int_0^1 dx \frac{5x^4 (1-x^2)^2 \varphi^2(x)}{z^2 (z^2 - 1) (1-x^2)^2 (\varphi(x) - \lambda x^2)^2 + x^8 \tanh^2\left(\frac{z}{2}y\right) \eta^2}, \quad (77)$$

where

$$V_F = 0.36 \frac{M}{M^*} \left(\frac{n_p}{n_0}\right)^{1/3} \quad (78)$$

is the proton Fermi velocity; and  $n_0 = 0.16 \text{ fm}^{-3}$  is the number density of saturated nuclear matter.

By adding the contribution (54) caused by the axial-vector coupling we finally obtain the following total emissivity:

$$Q = Q_V^{\text{RPA}} + Q_A \quad (79)$$

with  $Q_V^{\text{RPA}}$  given by Eq. (77) and

$$Q_A = 1.17 \times 10^{21} \tilde{C}_A^2 \mathcal{N}_\nu \left( \frac{M^*}{M} \right)^2 \left( \frac{M^{*2}}{M^2} + \frac{11}{42} \right) V_F^3 \left( \frac{T_c}{10^9 \text{ K}} \right)^7 \times \\ \tau^7 y^7 \int_1^\infty \frac{z^5}{[\exp(zy) + 1]^2 \sqrt{(z^2 - 1)}} dz \quad (80)$$

## VI. NUMERICAL ESTIMATE

To evaluate emissivities (77), (80) numerically we use the analytic fit of the energy gap suggested in [6]:

$$y(\tau) = \sqrt{1 - \tau} \left( 1.456 - \frac{0.157}{\sqrt{\tau}} + \frac{1.764}{\tau} \right), \quad (81)$$

The number density of paired protons  $N_p$  depends on the dimensionless temperature  $\tau$ . By the use of the fitted temperature dependence for the energy gap (81) one can calculate  $N_p(\tau)$  as follows [12]:

$$\frac{N_p(\tau)}{n_p} = 1 + 2 \int \frac{df(E)}{dE} d\epsilon, \quad (82)$$

where  $E = \sqrt{\epsilon^2 + \Delta^2}$ , and  $f(E) = 1/(\exp(E/T) + 1)$ .

Thus, we obtain:

$$\lambda = \frac{\mu_e}{3M^*} \frac{N_p(\tau)}{n_p} \quad (83)$$

The function  $N_p(\tau)/n_p$  is shown in Fig. 4. For illustration we consider matter with total baryon density  $\rho = 2\rho_0$  consisting on neutrons with a small fraction of protons and electrons corresponding to  $\beta$ -equilibrium. We set the effective proton mass  $M^* = 0.7M^*$ . To

demonstrate efficiency of the collective effects, the  $Q_V^{\text{RPA}}$ , given by Eq. (77), is plotted in Fig. 5 versus the dimensionless temperature  $\tau = T/T_c$  together with that obtained by the loop approximation (LA) without collective effects. One can see that, the collective effects substantially enhance, the  $\nu\bar{\nu}$  emissivity caused by the vector weak current of protons, but the temperature dependence becomes more sharp. Due to the collective effects the total emissivity sharply increases when the temperature becomes below than the critical temperature for proton pairing. The temperature dependence of total emissivity is shown in Fig. 6. As mentioned above, when the chemical potential of electrons is larger than the muon mass, the nuclear matter contains muons. In this case the muonic contribution to the RPA polarization tensor can be taken into account as indicated in Eq. (64). The total emissivities calculated with and without the muon contribution are plotted in Fig. 7. The calculation was made under the condition for chemical equilibrium  $\mu_\mu = \mu_e$ .

## VII. EFFICIENCY OF NEUTRINO EMISSION DUE TO PROTON PAIRING

The effect of neutron superfluidity and/or proton superconductivity on different neutrino reactions in the neutron star core is very complicated. Different neutrino production mechanisms can dominate at different cooling stages depending on the temperature, and the matter density, and vary along with the chosen parameters  $T_{cp}$ ,  $T_{cn}$ , which are the critical temperatures for the proton and neutron pairing. Fig. 8 shows efficiency of different reactions at the baryon density  $\rho = 2\rho_0$ , where the Direct Urca process is forbidden. Neutrino emissivities due to the singlet-state proton pairing, and the triplet-state neutron pairing are plotted in logarithmic scale against the temperature together with the total emissivity of two branches of the modified Urca processes, and the total bremsstrahlung emissivity caused by nn-, np-, and pp-scattering, which are suppressed due to the neutron superfluidity and/or proton superconductivity (See [14], [15], [16]). Two panels of Fig. 8 differ only by different choice of parameters  $T_{cp}$  and  $T_{cn}$ . On the left panel we took  $T_{cp} = 5.6 \times 10^8$  K, as calculated in [17] for  $\beta$ -equilibrium nuclear matter, and  $T_{cn} = 5.6 \times 10^9$  K, as obtained in. [18] for

triplet-state neutron pairing. On the right panel we assume  $T_{cp} = 3.5 \times 10^9$  K - the result obtained in [19], and  $T_{cn} = 8.5 \times 10^8$  K, as suggested in [20]. Partial contributions of the proton and neutron pairing to the total energy losses are very sensitive to the corresponding critical temperatures. Unfortunately the critical temperatures  $T_{cp}$  and  $T_{cn}$  are not well known up to now. Different authors [17] - [22] suggest  $T_{cp}$  and  $T_{cn}$  which vary in the wide range from  $10^8$  to  $10^{10}$  K and sensitively depend on the model of strong interactions used for calculation. A large scatter of  $T_{cp}$  and  $T_{cn}$  does not allow to make choice among many different microscopic results for these parameters. Therefore, considering the critical temperatures as free parameters, in Fig. 9, we show the regions of  $T_{cp}$  and  $T_{cn}$ , where different neutrino mechanisms dominate. Additionally to neutrino mechanisms considered above we have included neutrino bremsstrahlung due to electron-electron collisions recently calculated by Kaminker and Haensel [23]. Unfortunately, their calculation for neutrino emissivity does not take into account the collective effects, which substantially modify the effective vector weak current of the in-medium electron [24]. However, one can hope that the reappraised result will be of the same order of magnitude, and the difference will not be significant in the logarithmic scale we use.

Two panels of Fig. 9 illustrate the case of the standard cooling at  $\rho = 2\rho_0$  for two internal temperatures of the neutron star:  $10^8$  and  $6 \times 10^8$  K. Our calculations show that the represented diagrams does not vary noticeably with the matter density in the region, where the proton superconductivity exists. Thus, the diagrams of Fig. 9 show the efficiency of the neutrino production due to proton singlet-state pairing in the cooling neutron star. One can see that there are wide regions in the diagrams, where the singlet-state proton pairing dominates in neutrino production.

## VIII. SUMMARY AND CONCLUSION

We have calculated the neutrino-pair emissivity caused by a singlet-state Cooper pairing of protons by taking into account electromagnetic correlations among the charged particles

in a QED plasma. To incorporate the electromagnetic correlations we applied the Random phase approximation and derived Eq. (77) for contribution of the vector weak current to the neutrino emissivity. We found that, virtual electron excitations, electromagnetically induced by protons undergoing the quantum transition, generate neutrinos coherently with the initial protons and lead to stronger neutrino emission than that calculated by different authors without taking into account the plasma effects. Partial contribution of the proton reaction to the energy losses from the neutron star is very sensitive to the critical temperatures for the proton and neutron pairing. Unfortunately the critical temperatures  $T_{cp}$  and  $T_{cn}$  are not well known up to now. Their theoretical values sensitively depend on the model of strong interactions used for calculation and vary in the wide range from  $10^8$  to  $10^{10}$  K. In Fig. 9, for the temperatures interesting for practice, we show the regions of  $T_{cp}$  and  $T_{cn}$ , where different neutrino mechanisms dominate. The represented diagrams does not vary noticeably with the matter density in the region, where the proton superconductivity exists, and demonstrate wide domains in the plane  $T_{cn}, T_{cp}$ , where the singlet-state proton pairing dominates in the neutrino production.

### ACKNOWLEDGMENTS

This work was supported by Spanish Grant DGES PB97- 1432, and the Russian Foundation for Fundamental Research Grant 00-02-16271.

**APPENDIX A: NUCLEAR RENORMALIZATION OF THE PROTON WEAK  
VERTEX**

Effect of nucleon-nucleon correlations was evaluated in [5]. Following this work (Eq. 2.20), the vector weak form-factor of the proton in nuclear matter is of the following form:

$$\kappa_{pp} = \tilde{C}_V - \frac{f_{np}A_{nn}}{1 - 2f_{nn}A_{nn}}, \quad (\text{A.1})$$

As we use the reduced coupling constants of the proton, the form-factor  $\kappa_{pp}$  differs by the factor of 1/2 from that obtained in [5]. We have also omitted the factors  $\tilde{C}_0$  and  $\tilde{C}_0^{-1}$  which finally cancel in the original expression given by the authors. Then, in the actual case of  $k \leq \omega \sim T$ , the quantity  $A_{nn}$  can be written as:

$$A_{nn}(\omega, k) = \frac{1}{2} \left( 1 - \frac{s}{2} \ln \frac{s+1}{s-1} \right) \quad (\text{A.2})$$

with  $s = \omega/kV_{Fn}$ .  $f_{np}, f_{nn} \sim 1$  are constants of the theory of finite Fermi systems.

As the above calculation was made for the case of non-relativistic neutrons we have to assume that the Fermi velocity of neutrons  $V_{Fn} \ll 1$ . Thus, we have  $s \gg 1$ . In this limit

$$A_{nn}(\omega, k) \simeq -\frac{1}{6s^2} \ll 1 \quad (\text{A.3})$$

and the vector weak form-factor of the proton can be simplified as follows

$$\kappa_{pp} \simeq \tilde{C}_V + \frac{f_{np}}{6s^2}. \quad (\text{A.4})$$

The constants of the theory of finite Fermi systems are not very good known for the  $\beta$ -equilibrium nuclear matter. However, even assuming in the order of magnitude  $f_{np} \sim 1$  we obtain  $\kappa_{pp} \sim \tilde{C}_V$ . Thus, the renormalized proton vector weak coupling is found to be much smaller than that for electrons. Therefore the nuclear renormalization effects are negligible with respect to the plasma effects under consideration. A small nuclear correction to the axial-vector weak coupling of protons can also be neglected.

## REFERENCES

- [1] E. Flowers, M. Ruderman, P. Sutherland, *ApJ* 205 (1976) 541.
- [2] C. Shaab, D. Voskresensky, A. D. Sedrakian, F. Weber, M. K. Weigel *A&A*, 321 (1997) 591.
- [3] D. Page, In: *Many Faces of Neutron Stars* (eds. R. Buccheri, J. van Peredijis, M. A. Alpar. Kluwer, Dordrecht, 1998) p. 538.
- [4] D. G. Yakovlev, A. D. Kaminker, K. P. Levenfish, In: *Neutron Stars and Pulsars* (ed. N. Shibasaki et al., Universal Academy Press, Tokio, 1998) p. 195.
- [5] D. N. Voskresensky, and A. V. Senatorov, *Yad. Fiz.* 45 (1987) 657 [*Sov. J. Nucl. Phys.* 45 (1987) 411].
- [6] D. G. Yakovlev, A. D. Kaminker, K. P. Levenfish, *A&A* 343 (1999) 650.
- [7] A. D. Kaminker, P. Haensel, and D. G. Yakovlev, *A&A* 345 (1999) L14.
- [8] T. Takatsuka, R. Tamagaki, *Progr. Theor. Phys. Suppl.* 112 (1993) 27.
- [9] L. B. Leinson, *Phys. Lett. B* 473 (2000) 318.
- [10] E. Braaten and D. Segel, *Phys.Rev. D* 48 (1993) 1478.
- [11] E. M. Lifshitz, L. P. Pitaevskii, *Physical Kinetics*, (Pergamon Press, Oxford, 1981).
- [12] E. M. Lifshitz, L. P. Pitaevskii, *Statistical Physics., Part 2* (Pergamon Press, Oxford, 1980).
- [13] A. B. Migdal, *Theory of Finit Fermi Systems and Properties of Atomic Nuclei* [in Russian] ( Nauka, Moscow, 1983); English translation of earlier eddition: *Theory of Finit Fermi Systems* (Interscience, New York, 1967).
- [14] K. P. Levenfish, D. G. Yakovlev, *Strongly Coupled Plasma Physics* (Eds H. M. Van Horn, S. Ichimaru, Univ. of Rochester Press, Rochester, 1993,) p. 167.

- [15] K. P. Levenfish, D. G. Yakovlev, *Astron. Reports* 38 (1994) 247.
- [16] K. P. Levenfish, D. G. Yakovlev, *Astron. Lett.* 20 (1994) 43.
- [17] L. Amundsen, E. Ostgaard, *Nucl. Phys. A* 442 (1985) 163.
- [18] M. Hoffberg, A. E. Glassgold, R. W. Richardson, M. Ruderman, *Phys. Rev. Lett.* 24 (1970) 775.
- [19] L. Amundsen, E. Ostgaard, *Nucl. Phys. A* 437 (1985) 487.
- [20] M. Baldo, J. Cugnon, A. Lejeune, U. Lombardo, *Nucl. Phys. A* 536 (1992) 349.
- [21] R. Tamagaki, *Prog. Theor. Phys.* 44 (1970) 905.
- [22] T. Takatsuka, R. Tamagaki, *Prog. Theor. Phys.* 112 (1993) 27.
- [23] A. D. Kaminker, P. Haensel, *Acta Phys. Polonica* 30 (1999) 1125.
- [24] L. B. Leinson, *Phys. Lett. B* 469 (1999) 166.

## FIGURES

FIG. 1. Feynman graphs contributing to polarization of the proton plasma. Two proton loops, in the right-hand side, are contributions from the normal quasi-particle propagator and from "so-called" anomalous propagator which arises in the superconducting phase.

FIG. 2. The graphical representation for the Dyson's equation. The in-medium photon, shown by thick dashed line, is the infinite sum of ring particle-hole diagrams, connected by thin dashed line of the massive photon in the superconductor.

FIG. 3. The graphical representation for the RPA polarization tensor. The in-medium photon, shown by thick dashed line, is a solution of the Dyson equation collecting the infinite sum of ring particle-hole diagrams, connected by the line of the massive photon in superconductor.

FIG. 4. Relative fraction of paired protons  $N_p/n_p$  versus the dimensionless temperature  $\tau = T/T_c$

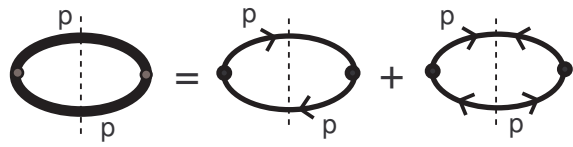
FIG. 5. Temperature dependence of the RPA vector weak current contribution to neutrino emissivity in comparison with that obtained in the loop approximation (LA). The emissivities shown versus the dimensionless temperature  $\tau = T/T_c$  for  $\beta$ -equilibrium nuclear matter.

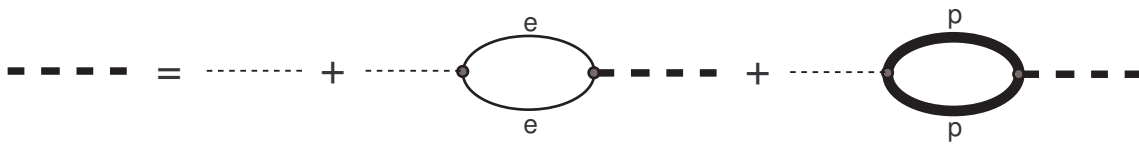
FIG. 6. Total emissivity  $Q = Q_V^{\text{RPA}} + Q_A$  versus the dimensionless temperature.

FIG. 7. Temperature dependence of the neutrino emissivity in different reactions for  $\beta$ -equilibrium nuclear matter of the density  $\rho = 2\rho_0$ . The neutrino emissivity due to the triplet-state neutron pairing is shown by dashed line. The solid line is the neutrino emissivity due to the singlet-state proton pairing. Dot-and-dash line shows the total bremsstrahlung emissivity caused by nn-, np-, and pp-scattering; the dotted line exhibits the total emissivity of two branches of the modified Urca processes. On the left panel we took  $T_{cp} = 5.6 \times 10^8$  K, and  $T_{cn} = 5.6 \times 10^9$  K. On the right panel we assume  $T_{cp} = 3.5 \times 10^9$  K, and  $T_{cn} = 8.5 \times 10^8$  K.

FIG. 8. Total neutrino emissivity calculated with and without the muon contribution.

FIG. 9. Regions of  $T_{cp}$  and  $T_{cn}$ , in which different neutrino reactions dominate at  $T = 10^8$ , and  $6 \times 10^8$  K in matter of the density  $\rho = 2\rho_0$





$$\begin{aligned}
 \Pi_V^{\text{RPA}} = & \tilde{C}_V^2 \text{ (p-p loop) } + c_V^2 \text{ (e-e loop) } - \text{ (e-e loop) } + \tilde{C}_V c_V \text{ (p-p loop) } - \text{ (e-e loop) } \\
 & + \tilde{C}_V c_V \text{ (e-p loop) } - \text{ (p-p loop) } + \tilde{C}_V^2 \text{ (p-p loop) } - \text{ (p-p loop) }
 \end{aligned}$$

